2017-02

FMCW Signal Detection and Parameter Extraction by Cross WignerHough Transform

Erdogan, A. Yasin; Gulum, Taylan O.; Durak-Ata, Lütfiye; Yildirim, Tülay; Pace, Phillip E.

IEEE

FMCW Signal Detection and Parameter Extraction by Cross Wigner–Hough Transform

A. YASIN ERDOGAN, Member, IEEE
TAYLAN O. GULUM, Member, IEEE
Turkish Naval Research Center Command, Istanbul, Turkey

LÜTFIYE DURAK-ATA, Senior Member, IEEE
İstanbul Technical University Informatics Institute, Istanbul, Turkey

TÜLAY YILDIRIM, Member, IEEE
Department of Electronics and Communication Engineering, Yildiz Technical University, Istanbul, Turkey

PHILLIP E. PACE, Fellow, IEEE
Department of Electrical and Computer Engineering, Naval Postgraduate School, Monterey, CA, USA

The combination of Wigner–Ville distribution (WVD) and Hough transform (HT) has been successfully used in detection and parameter extraction of frequency modulated continuous waveform (FMCW) signals. In this paper, a combination of Cross–Wigner–Ville and HT [(Cross Wigner–Hough transform (XWHT)] is proposed for detection and parameter extraction of FMCW signals with a novel methodology. The XWHT method makes use of the cross-terms created by WVD instead of trying to suppress them. Utilization of the properties of the cross-terms to detect and unveil the parameters of FMCW signals on HT space is a new approach. The performance of the method is compared with other Wigner–Hough transform-based methods in terms of transform speed, parameter extraction, and detection performance. As a result, this study proposes that the XWHT is a candidate method to be used in digital electronic support receivers' automatic signal detection and analysis capabilities due to its speed and performance.

I. INTRODUCTION

Military radar systems need to detect before being seen in order to gain an operational superiority over the opponent's noncooperative intercept receiver [1]. Therefore, frequency modulated continuous waveforms (FMCW) and other low probability of intercept (LPI) radar waveforms are widely used in contemporary radar systems because of their low power and wideband properties [2].

To analyze the nonstationary signals, like FMCW signals, time–frequency (TF) signal representations are needed. The main motivation of TF distributions is to devise a joint function of time and frequency that describes the energy of the signal in both time and frequency. A successful application of TF distribution requires prior knowledge about the signal so that the most suitable distribution is selected [3]. In this paper, Wigner–Ville Distribution (WVD) is chosen as the TF distribution since; it gives the highest energy concentration in TF plane, exhibits the nonstationary properties of the signals, and satisfies the marginal conditions [4].

When the signal to be analyzed is composed of more than one component; WVD presents signal autoterms as positive amplitudes along their instantaneous frequency lines and the cross-terms as oscillatory amplitudes at the geometrical midpoint of autoterms [5]. The cross-term problem of the WVD was first pointed out in [6]. The literature is rich in terms of studies to suppress the cross-terms and enhance the TF resolution; in [5], amplitude modulation of the cross-terms was used to reduce them in Wigner–Hough Transform (WHT). Poyil *et al.* in [7] detect the linear frequency modulation (LFM) signal components in Hough Transform (HT), then using the parameters of these components, they use back estimation to filter out only the signal components in WVD. Another study investigated the use of TF-based blind source separation technique for elimination of cross-terms in WVD [8]. Researchers proposed a method called standardization of the pseudoquadratic form to eliminate the cross-terms in [9].

The existence of cross-terms, however, is not always to be avoided; there are several studies in the literature that make use of WVD cross-terms in different research areas. It has been used in WVD-based radar processors to detect the presence of targets in [10]. In a medical application, WVD cross-terms were used to detect presence of very small signal terms, ventricular late potentials, in patients who have suffered heart attacks [11]. However, the use of WVD cross-terms, especially on HT space, has not been presented in radar signal interception methods. In this paper, we propose the Cross Wigner–Hough Transform (XWHT) method to detect and unveil the parameters of the FMCW signals on HT space by utilizing the properties of the cross-terms.

In Section II, we start with explaining the WVD and WVD cross-terms. Section III introduces the commonly used FMCW LPI waveform and explains the general approach for WHT-based FMCW detection and parameter extraction. We also summarize the legacy HT in this section

and mention about the improvements on it. Section IV introduces the XWHT method and analyzes its performance. Finally, Section V concludes the work by stating that the XWHT is a candidate method that can improve electronic support receivers (ESRs') automatic signal detection and analysis capabilities with its speed and performance.

II. WIGNER–VILLE DISTRIBUTION

WVD was first proposed by Wigner with the motivation to devise a joint distribution that gave the quantum mechanical distributions of position and momentum simultaneously [12]. But it was Ville who introduced WVD into signal analysis with his work in [13].

A. WVD Representation

Continuous WVD of a signal $s(t)$ can be calculated with the following integral:

$$W_s(t, w) = \frac{1}{2\pi} \int s\left(t - \frac{1}{2}\tau\right) \times s^*\left(t + \frac{1}{2}\tau\right) e^{-j\tau w} d\tau \tag{1}$$

where w is the frequency variable, t is the time variable, and τ is the time lag [14].

B. WVD Cross-Terms

The creation of cross-terms can be explained as two points of the TF space interfering to create a contribution on another point at their geometrical midpoint. These cross-terms have positive and negative amplitude values, they are amplitude modulated, have zero mean [15], and their amplitudes are higher than the signal components' amplitudes [16]. Assuming signal $s(t)$ is composed of two signal components $s(t) = s_1(t) + s_2(t)$, WVD of $s(t)$ can be calculated as [14]

$$
\begin{aligned}
W_s(t, w) = \frac{1}{2\pi} \Bigg[&\overbrace{\int s_1\left(t - \frac{1}{2}\tau\right) \times s_1{}^*\left(t + \frac{1}{2}\tau\right) d\tau}^{W_{s1s1}(t,w)} \\
&+ \overbrace{\int s_1\left(t - \frac{1}{2}\tau\right) \times s_2{}^*\left(t + \frac{1}{2}\tau\right) d\tau}^{W_{s1s2}(t,w)} \\
&+ \overbrace{\int s_2\left(t - \frac{1}{2}\tau\right) \times s_1{}^*\left(t + \frac{1}{2}\tau\right) d\tau}^{W_{s2s1}(t,w)} \\
&+ \underbrace{\int s_2\left(t - \frac{1}{2}\tau\right) \times s_2{}^*\left(t + \frac{1}{2}\tau\right) d\tau}_{W_{s2s2}(t,w)} \Bigg] \int e^{-j\tau w} d\tau.
\end{aligned}
\tag{2}
$$

In this expression $W_{s1s2}(t, w)$ and $W_{s2s1}(t, w)$ terms are called the Cross Wigner–Ville distribution [17]. Since $W_{s1s2} = W^*{}_{s2s1}$, we can rearrange (2) as [14]

$$W_s(t, w) = W_{s1s1}(t, w) + W_{s2s2}(t, w) + 2\mathrm{Re}\{W_{s1s2}(t, w)\} \tag{3}$$

where the last term corresponds to the cross-terms. If W_{s1} is around (t_{s1}, w_{s1}) and W_{s2} is around (t_{s2}, w_{s2}), then the cross-term lies midway between these signal terms [18]:

$$(t_x, w_x) = \left(\frac{t_{s1} + t_{s2}}{2}, \frac{w_{s1} + w_{s2}}{2}\right). \tag{4}$$

III. WHT-BASED FMCW DETECTION AND PARAMETER EXTRACTION

WHT translates the signals from time domain to a parameter space in which detection and parameter extraction of signals can be performed simultaneously [5]. This combination makes it possible to redefine the problem of detecting FMCW components in WVD as detecting the high-intensity points in HT space. The detection decision is given whenever the amplitude of any point in HT space exceeds the detection threshold, ζ.

A. FMCW Radar Signals

Conventional ESRs are generally tuned to detect pulse and CW waveforms, and LPI radars try to avoid interception by mismatching their waveforms to these waveforms [19]. Wideband linear FMCW is one of the most common waveform structures used to achieve LPI operations because of its ease in implementation, its versatility, and its suitability for fast FT processing to obtain range measurements [20]. The up/down chirp FMCW modulation consists of positive/negative slope LFM parts. The transmit signal expressions for positive and negative parts are given as [21]

$$s_{p,n}(t) = a_0 \cos\left(2\pi\left(\left(f_c \mp \frac{B}{2}\right)t \pm \frac{B}{2T_m}t^2\right)\right) \tag{5}$$

where f_c is the RF carrier frequency, B is the transmission modulation bandwidth, and T_m is the modulation time. The chirp rate of FMCW signals changes according to the radar's instrumented range and desired range resolution. Although the chirp rate is generally represented by the ratio ($\beta = T_m/B$), we represent it as an angle in this study.

Using the positive part of (5) and discrete pseudo-WVD (PWVD) formula given in [22], we present the geometric relations of FMCW modulation parameters on a two-component up-chirp FMCW signal's PWVD in Fig. 1.

PWVD is actually an $N \times M$ matrix, elements of which can be represented by

$$W(n_i, w_j), \quad i = 1, 2, \ldots, N; \quad j = 1, 2, \ldots, M. \tag{6}$$

We take $2M$ as the FFT length, N as the number of signal samples collected in the observation time (T_{obs}), f_{s1} as the sampling frequency, T_{s1} as the sampling interval, and f_c as carrier frequency.

On the y-axis, $f_{s1}/2$ is represented by M (positive Wigner spectrum), which gives us frequency resolution as $\Delta f_1 = f_{s1}/(2M)$ and on the x-axis T_{obs} is represented by N, where $T_{\mathrm{obs}} = N \times T_{s1}$.

B. Optimality of WHT for FMCW Detection

The optimality of WHT for detection of FMCW signals was explained in [23]. It was stated that if the position
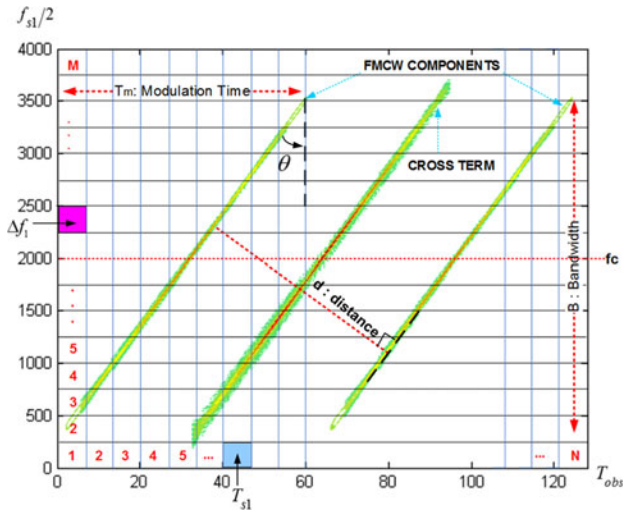
Fig. 1. Geometric relations of a two component upchirp FMCW waveform parameters on WVD.

Fig. 2. HT geometry shown on an $f(x, y)$ image.

and sweep rate of the linear chirp is not known, to perform generalized likelihood ratio test, one should integrate WVD along all the possible lines (instantaneous frequency lines) in the TF plane and the resulting peak value shall be compared against a threshold. We can assume that, at the output of the ESR, there is complex white Gaussian noise $n(t)$ ($\aleph(0, \sigma_n^2)$; 0 : zero-mean, σ_n^2 : variance) and the signal $s(t)$, if it exists (i.e., $r(t) = s(t) + n(t)$). To detect the signal $s(t; \chi)$ in additive white Gaussian noise (AWGN), ESR shall filter the intercepted $r(t)$ signal with a matched filter whose impulse response $h(t, \chi)$ is determined by signal parameters. Here, χ vector includes the maximum likelihood estimate of the signal parameters. If the parameters of the signal are not known *a priori*, maximum filter output is searched as a function of signal parameters and time delay. Assuming time delay is known, then the expression below can be compared against ζ to decide detection [5]:

$$\max_\theta \left| \int h(\tau; \chi) r(\tau) d\tau \right|^2. \tag{7}$$

By using the unitarity property of the WVD, time-domain square modulus of the scalar product in (7) can be represented as a scalar product of the WVDs in TF domain using Moyal's formula [5]

$$\max_\theta \iint W_h(t, f; \chi) W_r(t, f) dt df. \tag{8}$$

If we consider FMCW signals in AWGN, WVD of the impulse response of the filter to be used ($W_h(t, f; \chi)$) will have the form of FMCW. In this case, the double integral in (8) can be calculated using a line integral. Since the parameters of this line are not known *a priori*, the integral needs to be calculated for all the possible lines on WVD [5] and *this can be done by calculating HT of the WVD.*

C. HT and Improvements on HT

HT is a pattern recognition technique that is widely used in image processing to detect geometric shapes in images.
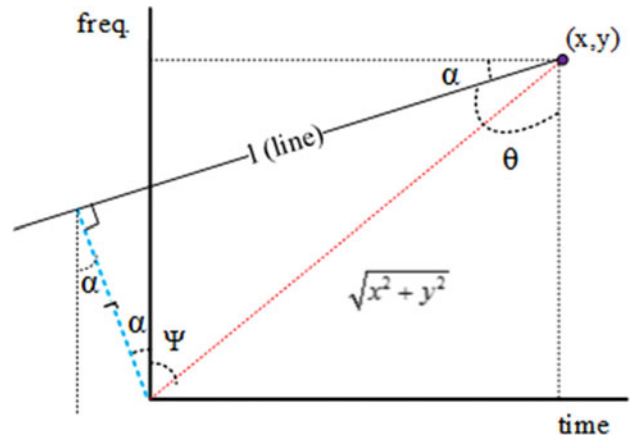
In an $f(x, y)$ image, we can represent a radial line l with its orthogonal distance r to the origin and with its normal's angle α, as shown in Fig. 2. (In this study we use θ in the formulations below instead of α, since we also define chirp rate by θ). This line corresponds to an (r, θ) point in HT space and transformed by the following formula:

$$r = x \sin\theta + y \cos\theta. \tag{9}$$

Distance r in (9) can be represented as a sinusoid with amplitude and phase dependent on the (x, y) coordinates [24]. If we transform each line crossing over an (x, y) point, we will have a sinusoid in HT space corresponding to the (x, y) point

$$\psi = \arctan\frac{x}{y}, \quad r = \sqrt{x^2 + y^2} \cdot \cos(\alpha + \psi). \tag{10}$$

WHT-based methods can be computationally expensive. Calculating the HT for only a limited set of chirp rates (signals of interest) and for WVD points exceeding TF threshold, $\mathrm{Th_{WD}}$, will reduce the required processing power and complexity. WHT [25], Wigner–Hough–Radon (WHRT) [26], and Modified Wigner–Hough (MWHT) [27] transforms were previously proposed to reduce the complexity, yet keeping FMCW parameter extraction performance above a certain level.

In WHT, all the lines passing over $(x_i, y_j) \in \{f(x_i, y_j) \geq \mathrm{Th_{WD}}\}$ points were transferred to (r, θ) space. Equation $x_i \sin\theta_l + y_j \cos\theta_l = r_k$ was used for transformation and the counter was increased by one for the corresponding (r_k, θ_l) point [25]:

$$C(r_k, \theta_l) = C(r_k, \theta_l) + 1. \tag{11}$$

A common (r_k, θ_l) coordinate was calculated for points on the same line. This common (r_k, θ_l) coordinate was observed as a high-intensity point in HT space.

In Wigner–Radon (WRT) method [28], the cross-terms in the WVD integrate to a relatively small value due to negative and positive oscillations present in their structure. It was proposed to implement WRT with a dual threshold (12) to exploit the cross-term minimization property of
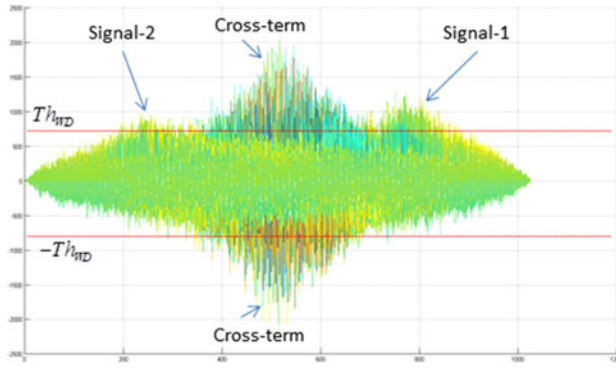
Fig. 3. WVD of a two Component FMCW up-chirp signal at –6 dB (X-Z view).

WRT, and this method was called WHRT. In this method, the intensity value I, was updated instead of counter, as follows [26]:

$$\text{if } (x_i, y_j) \in \left\{ f(x_i, y_j) \geq \text{Th}_{\text{WD}} \text{ or } f(x_i, y_j) \leq -\text{Th}_{\text{WD}} \right\}$$
$$\text{then } I(r_k, \theta_l) = I(r_k, \theta_l) + I\_\text{new}(r_k, \theta_l). \quad (12)$$

In MWHT, the counter was updated as shown in (13). This increased the counter for autoterms, and preserved the counter for cross-terms from increasing due to their oscillating intensity values [27]:

$$C(r_k, \theta_l) =$$
$$\begin{cases} C(r_k, \theta_l) + 1 \text{ if}(x_i, y_j) \in \left\{ f(x_i, y_j) \geq \text{Th}_{\text{WD}} \right\} \\ C(r_k, \theta_l) - 1 \text{ if}(x_i, y_j) \in \left\{ f(x_i, y_j) \leq -\text{Th}_{\text{WD}} \right\} \end{cases}. \quad (13)$$

IV. CROSS WIGNER–HOUGH TRANSFORM

The methods mentioned above try to suppress the cross-terms. However, the cross-terms obtain valuable information that can be used in radar signal interception efforts. They are necessary for unitarity property (i.e., Moyal's formula) to hold, which is important to derive a closed-form solution for FMCW signal analysis based on WHT methods [24]. In the literature, only a few works have been performed in radar signal detection area on the utilization of information contained in cross-terms. Cross-terms are deliberately formed between an analyzed signal and a reference signal in [29]. The method uses the geometrical properties of the cross-terms to estimate the instantaneous frequency of the analyzed signal. A similar method is used in [30] to suppress the cross-terms by multiplying the WVD with a 2-D mask. The mask was designed by exploiting the geometrical properties of the cross-terms created between the analyzed signal and reference signal. These methods use the properties of the cross-terms to exploit them on WVD space. In this paper, the XWHT method is proposed to make use of the properties of the cross-terms on HT space.

In Fig. 3, we present WVD of a two-component FMCW up-chirp signal at –6 dB SNR, where the high-intensity cross-term can easily be distinguished. We can see that the positive intensity part contains both the cross-term and signal components, whereas the negative intensity part contains only the cross-term. Therefore, the negative intensity

part is more appropriate for putting a threshold to discriminate cross-terms. With the choice of a best performing negative threshold ($-\text{Th}_{\text{XWD}}$), the counted lines will be those passing over points on the cross-terms.

Considering the properties of cross-terms, we propose to create a counter for only negative intensity values so that, the cross-terms inherent in WVD protrude significantly in HT. In this case, if $x_i \sin \theta_l + y_j \cos \theta_l = r_k$, than the counter is updated as

$$\text{if } (x_i, y_j) \in \left\{ f(x_i, y_j) \leq -\text{Th}_{\text{XWD}} \right\}$$
$$C(r_k, \theta_l) = C(r_k, \theta_l) + 1. \quad (14)$$

A. FMCW Parameter Extraction Using XWHT

For parameter extraction using any of the transform methods mentioned so far, we employ WVD to obtain TF images; these images are then transferred to a parameter space of (r, θ) by HT/RT. In this parameter space, the FMCW signals are detected first and then the properties of the signals are determined. This parameter space is calculated for all the θ values and we crop the vector at θ holding the peak value of the transform space to measure the orthogonal distance between signal components, d. Here, we propose another algorithm which automatically detects FMCW signal components and performs parameter extraction using XWHT. Our goal in this method is to find θ with XWHT as soon as possible and then calculate d. After detecting the FMCW signal and its θ, we need the HT of signal components to calculate d. At this point, HT is employed for only this specific θ, determined by XWHT. Then, we obtain two vectors for the same θ; XWHT(θ) vector holding the cross-term and WHT(θ) vector holding both the signal components and the cross-term. It will be shown in the next section that the transform speed of the XWHT is much higher than other HT/RT-based methods. Determining the θ of the signal with this very fast method and then calculating the computationally expensive HT for only one θ is the main advantage of the proposed method. The flow diagram of the algorithm is shown in Fig. 4.

We analyze the performance of the method using the signals in Table I.

The signals are modeled in ten different SNR levels (9, 6, 3, 0, –3, –6, –7, –8, –9, –10 dB) to simulate different ranges, and low-sampling frequency is used for ease of simulations ($f_s = 8 \text{ kHz}$). In order to fit at least two signal components in 1024 sample length time, $T_m = 64 \text{ m} \cdot \text{s}$ is used for all signals. Monte Carlo runs are performed 100 times for each SNR level.

Top graph in Fig. 5 shows the effect of noise and cross-term on the WHT(θ) vector. Obviously, the correct calculation of d depends on avoiding the effects of noise and cross-terms.

Considering that XWHT is actually WHT with only negative threshold, subtracting XWHT vector from WHT vector suppresses cross-term and noise effect and it gives us a rather clear vector for calculating d. The middle graph shows the XWHT(θ) vector and the bottom graph illustrates the result of the vector subtraction for S1($\cdot$) at –12 dB SNR.
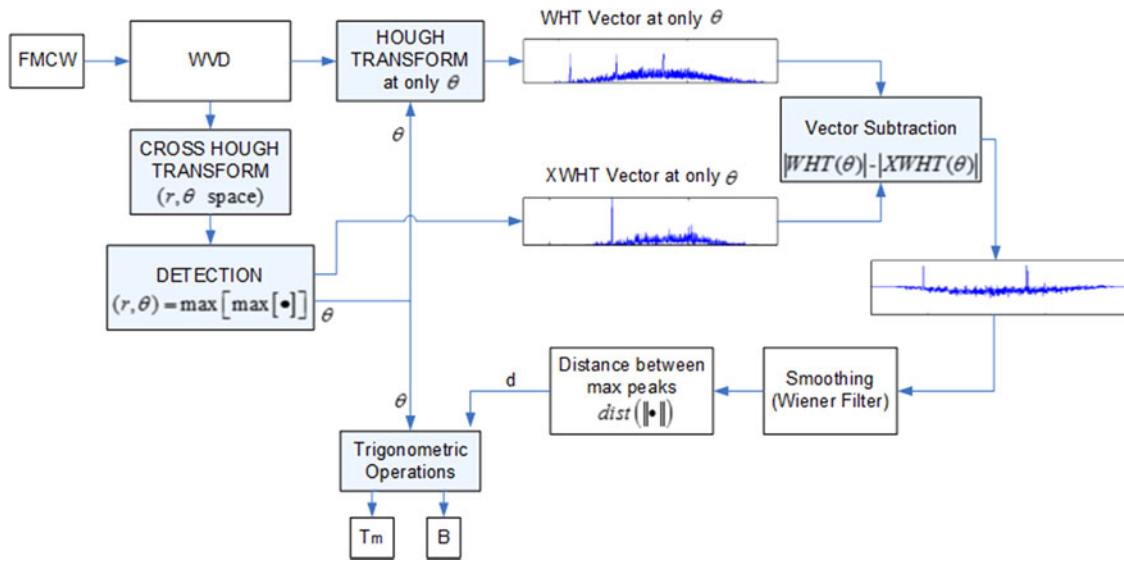
Fig. 4.   Proposed detection and parameter extraction algorithm flow diagram using XWHT.

TABLE I
Test Signal Database

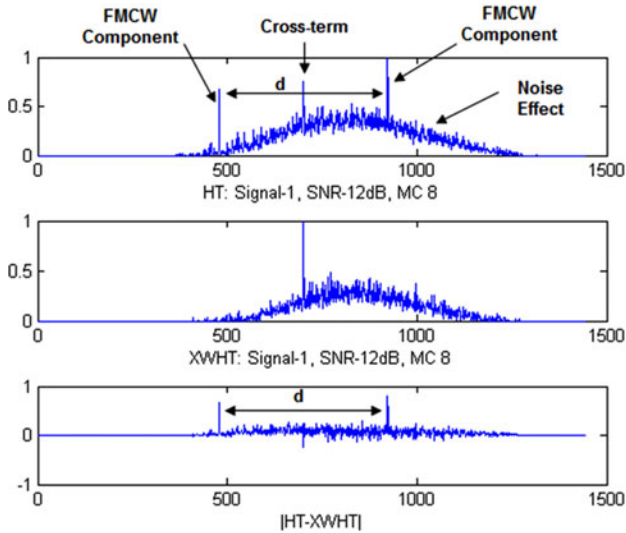| Signals	Chirp rate	B (in terms of fs)	f_c(Hz)
Signal 1 (S1)	30	0.433	$f_s/4$
Signal 2 (S2)	45	0.25	
Signal 3 (S3)	60	0.144	
Signal 4 (S4)	75	0.067	

Fig. 5.   Top: WHT vector, Middle: XWHT vector, Bottom: |WHT-XWHT| Vector for S1(·) at –12 dB SNR.

Once we get d and θ, the FMCW characteristic parameters are extracted by using the formulas in (15) for all the HT/RT-based methods, including XWHT. Therefore, XWHT's performance of deriving d and θ, along with its transform speed, are used as means of comparison with

other transform methods, in the next section

$$B = \frac{d}{\cos \alpha} \text{ for } (\theta_0 > 90°), B = \frac{d}{\sin(\alpha - 90)} \text{ for } (\theta_0 < 90°)$$

$$T_m = \frac{B}{\tan(\alpha)}. \tag{15}$$

B. Performance Analysis of XWHT-Based Parameter Extraction

In this section, we analyze the efficiency of XWHT method by comparing it with the other WHT-based parameter extraction methods in terms of; parameter extraction performance and transform speed. $N = 1024$ sample length signals, $M = 1024$ FFT bins (positive frequency bins) are used and at least two up-chirp FMCW signal components are simulated. We assume that best performing Th_{WD} is chosen for each method. Best performing Th_{WD} interval for extracting FMCW signal parameters using WHT-based methods was investigated in [27]. In this investigation; WHT-based algorithms were found to perform well with Th_{WD} values chosen between 20%–40% of the maximum WVD intensity levels of the signal.

Before performance comparison, the best performing Th_{WD} for XWHT is derived. XWHT tries to increase the intensities of cross-terms more than auto-terms' in HT space. So, considering the properties of cross-terms, a smaller negative threshold on WVD is thought to increase the probability of detection of cross-terms and to increase transform speed, i.e., shorten detection time. To find the best performing Th_{WD} for the chosen chirp rate estimation performance (P_{CRE}) using XWHT, we changed Th_{WD} in the interval of 20%–65% factors in 5% steps. Fig. 6 presents the result of this analysis at –10 dB SNR, where the threshold factor 40% makes P_{CRE} 100% for all test signals.

The effect of $-Th_{WD}$ for higher SNR levels (–9–0 dB) was also investigated. We have seen that for SNR levels
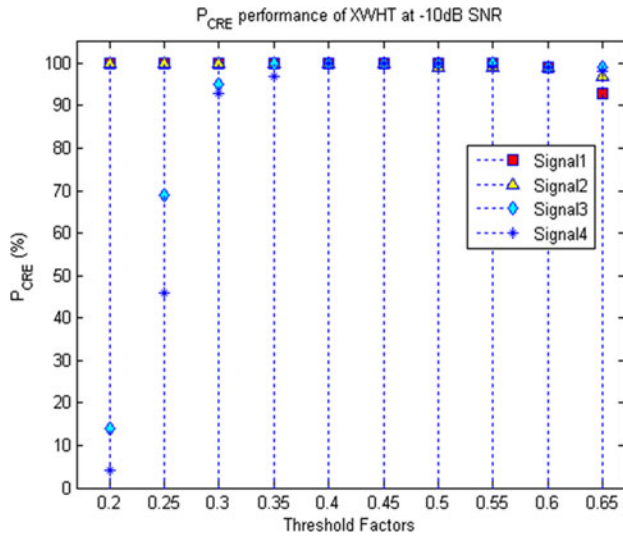
Fig. 6. P_{CRE} Performance of XWHT versus varying WVD threshold factors.
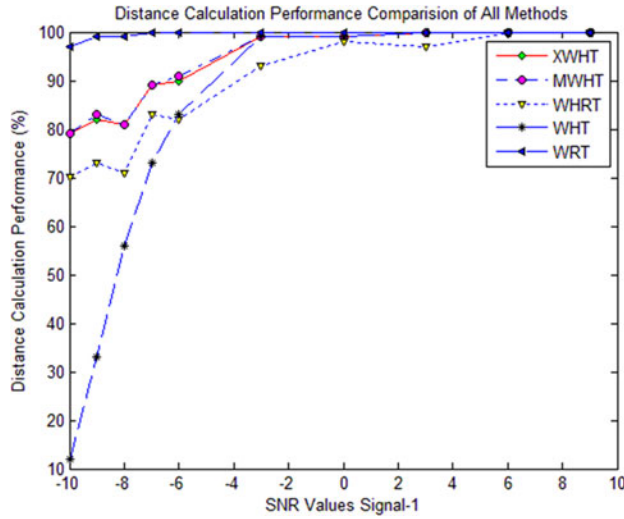

Fig. 8.   Transform speeds for $S1(\cdot)$.

Fig. 7.   Orthogonal distance calculation performance of transform methods.

−9 dB and higher, and for all test signals, we get P_{CRE} 100% when $-\mathrm{Th_{WD}}$ level is between 35%–45%. So, we concluded that we can use $-\mathrm{Th_{XWD}} = -0.4 \times \max[\mathrm{WVD}]$ both for low and high SNR levels.

1) Orthogonal Distance Calculation Performance: Fig. 7 shows the distance calculation performance of all the methods using $S1(\cdot)$ as an example signal. Similar results were derived for all the test signals. We can see that WRT gives us the best parameter extraction performance and XWHT and MWHT algorithms are next best.

2) Chirp Rate Estimation Performance: We have also looked at P_{CRE}. Finding the chirp rate in $\pm 1°$ tolerance was accepted as successful estimation. The simulation results are not presented here since it was seen that all methods performed with 100% success in finding the chirp rate down to –10 dB SNR levels.

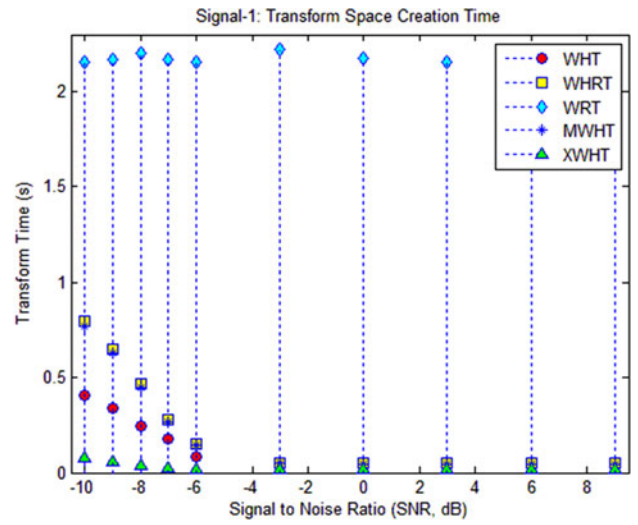*3) FMCW Parameters Extracted by XWHT*: In this study, the chirp rate estimation performance (P_{CRE}) shown

in Fig. 6 and orthogonal distance calculation performance (*d*) shown in Fig. 7 implicitly suggests the parameter extraction accuracy of the method, because once we get *d* and θ, the FMCW characteristic parameters are deterministically computed by using (15). So, it is fair to say that the accuracy in the calculation of *d* and θ directly determines the accuracy of the signal parameters, such as center frequency, bandwidth, and modulation time.

The algorithm works in such a way that, after the vector subtraction $|\mathrm{WHT}(\theta)| - |\mathrm{XWHT}(\theta)|$ shown in Fig. 5, we get a very clear vector for the calculation of *d*. However, depending on the SNR level, even if the cross-term intensity is enough for detection process in the parameter space, the signal components' intensity levels may be buried under noise level. In this case, even after the vector subtraction, wrong *d* and θ values are found, therefore they are discarded.

Revisiting Fig. 7 for accuracy analysis, we can say that the XWHT method accurately calculates the parameters of 82% of the signals at –9 dB, 90% of the signals at –6 dB, and 99% of the signals for SNR levels –3 dB and above.

Orthogonal distance calculation performance analyses results presented by Fig. 7 favor WRT, but P_{CRE} analyses show that all methods are successful in finding chirp rate. However, we have to keep in mind that ESR systems need to operate very fast due to their time-critical missions. Therefore, we need a very fast method with reasonable performance metrics. So we need to compare the transform methods in terms of their transform speed performance as well.

4) Transform Speed Comparison: Transform speed can actually be considered as the related method's signal detection speed, since we search for the maximum intensity points in the transform spaces to declare detection.

As has been defined in Table I, each test signal used in this study was designed to represent a different chirp rate. Fig. 8 shows the transform speeds of methods for $S1(\cdot)$ for SNR levels (–10–9 dB). Transform speed comparisons were

performed for all the test signals and for each test signal, comparison results were similar to the ones illustrated in Fig. 8. As will be explained in the next paragraph, the transform speeds of the transform methods solely depend on the number of WVD points to be used for the transform computations and not on the chirp rate. As expected, Fig. 8 shows that the XWHT method has the fastest transform speed.

Transform space calculation time results can be supported by the computational complexity calculations. The signal length is taken as S, number of FFT bins is taken as $2S$, and the number of angles for transforms is taken as F. Since WRT uses all the S^2 pixels in the WVD image, the computational complexity of WRT will be $O(FS^2)$. The computational complexity for WHT and WHRT is $O(FK)$, where $K < S^2$, because we only use $(x_i, y_j) \in \{f(x_i, y_j) \geq \text{Th}_{\text{WD}}\}$. For MWHT, the computational complexity is $O(FL)$, where $K < L < S^2$, because we use $(x_i, y_j) \in \{f(x_i, y_j) \geq \text{Th}_{\text{WD}}$ and $f(x_i, y_j) \leq -\text{Th}_{\text{WD}}\}$, and for XWHT, since it uses only $(x_i, y_j) \in \{f(x_i, y_j) \leq -\text{Th}_{\text{XWD}}\}$, the computational complexity is $O(FJ)$, where $J < K < L < S^2$ and $J \langle\langle S^2$, because only the cross-term magnitudes exceed $-\text{Th}_{\text{XWD}}$ and $|\text{Th}_{\text{WD}}| < |\text{Th}_{\text{XWD}}|$.

As a result we can conclude that XWHT method is a much faster transform method with a very good parameter extraction performance.

C. FMCW Detection Using XWHT

In the previous section, we have analyzed the performance of transform methods assuming that the signal was present in the intercepted data. The analyses were performed with a comparison focus and they showed that XWHT produced results much faster than the other transform methods mentioned in this paper. In this section, we try to compare the actual performance metrics of Wigner-Hough-Based FMCW detection methods; probability of detection (P_d) for a given probability of false alarm (P_{fa}). The investigation is performed on ROC curves of the WHT methods.

Although there are some studies in the literature to determine performance standards of ESRs [31], [32], there is still no globally accepted performance standard for ESR development. Also, there is a large difference between the theoretical and practical performance metrics of ESRs if generally accepted performance metrics like Cramer–Rao bound are used [33]. This is because generally accepted receiver performance metrics are suitable for communication receivers where properties of the received signal are known and there is an efficient receiver for the cooperative incoming signal. However, this is not the case for ESRs where the parameters of the incoming signal are not known. Since the performance metrics will be receiver dependent, we choose to perform numerical analysis for the WHT-based detection performance analysis instead of deriving analytic expressions. In order to avoid any unintentional misleading

	Chirp rate	B (in terms of fs)	fc
Signal 1	30	0.433	$f_s/4$
Signal 2	35	0.357	
Signal 3	40	0.298	
Signal 4	45	0.25	
Signal 5	50	0.209	
Signal 6	55	0.175	
Signal 7	60	0.144	
Signal 8	65	0.117	
Signal 9	70	0.091	
Signal 10	75	0.067	

performance reports, we only perform performance analysis by comparing our own methods with each other.

For this analysis, a more comprehensive FMCW signal database is used as shown in Table II, to include signals between chirp rates $30°-75°$ in $5°$ steps.

All the signals were modeled in eight different SNR levels (–3, –4, –5, –6, –7, –8, –9, –10 dB) with same T_m value. Higher SNR values were not modeled since we know that signals with high SNR values are detected with a very high performance regardless of their chirp rate [25], [26], [27]. Monte Carlo runs were performed 100 times for each SNR level.

To investigate the P_d performance, first we found the maximum intensity value of the transform spaces of all intercepts to normalize the intercept transform spaces, including noise-only cases. We assumed that, in our simulated operational area, the most powerful signals are intercepted at 9 dB SNR. So, for each signal in Table II, we found the peak value of transform space of each simulation at 9 dB SNR. As a requirement for our simulated ESR, we wanted to have $P_{fa} = 10^{-4}$. To determine the ζ for this P_{fa}, we simulated 10^4 "noise only" intercepts. The histograms of these intercepts were calculated to see the maximum intensity value that only noise intercepts could get and this value determined ζ.

The average of highest peak intensity values of XWHT spaces for each signal at 9 dB SNR level was investigated and highest peak value was derived at chirp rate $45°$ as 150. Then, from the histograms of noise simulations, the maximum intensity value is found as $\zeta = 0.3838$. This ζ value was verified by controlling the maximum intensity value of all 10^4 noise simulations, which was 58 ($\zeta = 58/150 = 0.38$).

In Fig. 9, we present the P_d curves for $P_{fa} = 10^{-4}$, using each signal in Table II, at each SNR level.

In Fig. 9, more obvious for SNR < –8.5 dB, we see that we get the highest P_d between chirp rates $30°-50°$. As the SNR increases, the difference between P_d's based on the chirp rates diminishes. The major cause of the differences stems from the need to represent the WVD as a digital (rectangular) grid for calculations. In this representation geometry, for $45°$ chirp rate, almost each respective point on the LFM contributes to the XWHT peak in the transform
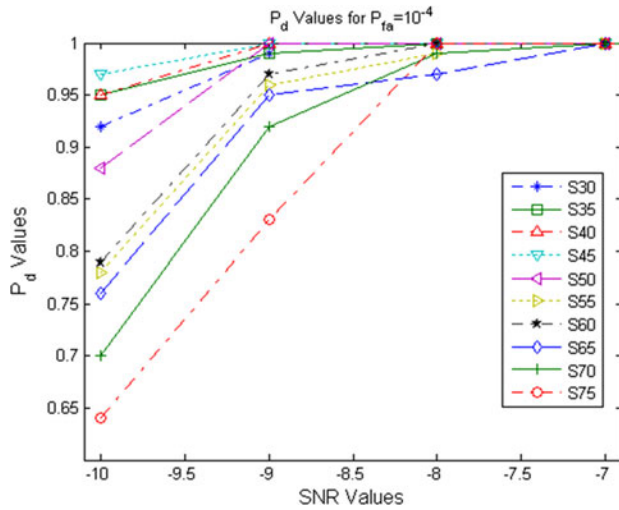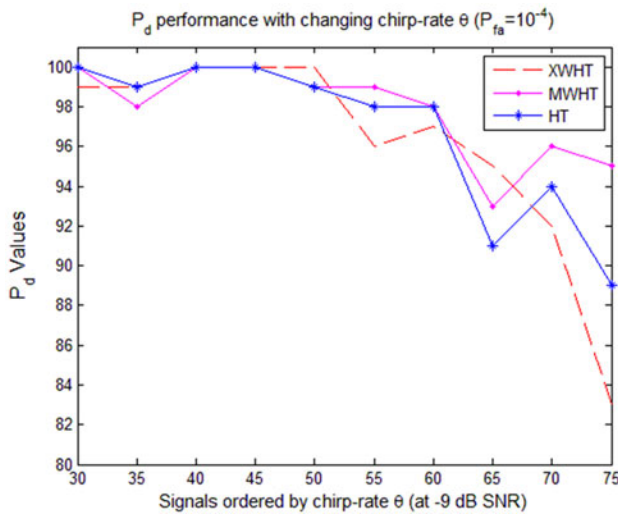
Fig. 9.   ROC: XWHT for $P_{fa} = 10^{-4}$.

Fig. 10. P_d Performance versus chirp rate (at –9 dB).

space. But when the chirp rate is above or below $45°$, the digital representation geometry sometimes calculates more than one point to be in the same WVD cell, causing the corresponding amplitudes in the transform space to subside. Since, above -8.5 dB SNR, enough LFM points from WVD are transferred to the XWHT space, component amplitudes exceed the Th_{XWD}, and chirp rate effect is not recognizable.

D. Performance Analysis of XWHT Based FMCW Detection

The same analysis is performed for MWHT and WHT methods as well. The P_d values of all WHT-based methods at –9 dB SNR are illustrated in Fig. 10. We can clearly see that the P_d performance of all WHT-based FMCW interception methods is considerably better between chirp rates $30° - 50°$.

As a result, the parameter extraction performance comparison in Section IV-B showed that XWHT provides a very good performance at the fastest time, and the detection performance comparison in Section IV-C showed that XWHT produces comparable detection performance between chirp

rates $30° - 50°$. Considering that it is also possible to digitally adapt the chirp rate to overcome the performance degradation for signals outside this chirp-rate interval [34], XWHT should be considered as a strong candidate to be applied in digital ESR systems.

V.   CONCLUSION

With more LPI systems coming into use, the signals of interest are changing at a rapid pace. ESRs currently in use are not well optimized for LPI signal detection. Interception of LPI signals requires sophisticated receivers that use TF signal processing, correlation techniques, and algorithms to overcome the processing gain of the LPI systems.

It is not always necessary for ESRs to have idealistic performance figures to achieve the dedicated task. ESRs process received signals over an observation period and perform detection without the need to have 100% P_d on every received signal.

Our goal in this study was to propose a candidate method to be used in ESRs for FMCW waveform detection and parameter extraction. We have exploited the properties of the cross-terms to detect and unveil the parameters of the FMCW signals on HT space using XWHT. We have compared the XWHT with other WHT-based methods in terms of speed, parameter extraction, and detection performance. Considering the performance analysis results, we can conclude that XWHT method produced very successful results in a much less processing time compared to other methods, which makes it a candidate method to be used in digital intercept receivers for FMCW waveform detection.

Future work will be on trying the XWHT on a much bigger database including poly-phase, poly-time coded signals, and hardware implementation with real radar waveform simulations.

REFERENCES

[1]   P. E. Pace
        To see and not be seen
        In *Detecting and Classifying Low Probability of Intercept Radar*, 2nd ed. Norwood, MA, USA: Artech House, 2009.

[2]   T. O. Gulum
        Autonomous nonlinear classification of LPI radar signal modulations
        M.S. thesis, Dept. Electron. Eng., Naval Postgraduate School, Monterey, CA, USA, 2007.

[3]   J. P. Stephens
        Advances in signal processing technology for electronic warfare
        IEEE Aerosp. Electron. Syst. Mag., vol. 11, no. 11, pp. 31–38, Nov. 1996.

[4]   L. Cohen
        Time-frequency distributions- A review
        Proc. IEEE, vol. 77, no. 7, pp. 941–981, Jul. 1989.

[5]   S. Barbarossa and A. Zanalda
        A combined Wigner-Ville and Hough transform for cross-terms suppression and optimal detection and parameter estimation
        In *Proc. IEEE Int. Conf. Acoust., Speech, Signal Process.*, 1992, vol. 5, pp. 173–176.

[6]   W. D. Mark
        Spectral analysis of the convolution and filtering of non-stationary stochastic processes
        J. Sound Vib., vol. 11, pp. 19–63, 1970.

[7] A. T. Poyil and S. A. Meethal
Cross-term reduction using Wigner Hough Transform and back estimation
In *Proc. Int. Conf. Ind. Control Electron. Eng.*, 2012, pp. 5–8.

[8] J. B. Wu, J. Chen, and P. Zhong
Time frequency-based blind source separation technique for elimination of cross-terms in Wigner distribution
Electron. Lett., vol. 39, no. 5, pp. 475–477, Mar. 6, 2003.

[9] Q. Li, T. Zhou, and W. Wang
New method to eliminate cross-term in Wigner Distribution
In *Proc. IET Int. Conf. Wireless, Mobile Multimedia Netw.*, 2006, pp. 1–3.

[10] J. Giridhar and K. M. M. Prabhu
Implementation details of MTD-WVD on a TMS320C30 DSP processor
Microprocessors Microsyst., vol. 22, no. 1, pp. 1–12, 1998.

[11] M. A. Reyna-Carranza, L. S. Fierro, and M. E. Bravo-Zanoguera
Wigner distribution's cross terms characterization to detect patterns of ventricular late potentials
In *Proc. Pan Amer. Health Care Exchanges*, 2012, pp. 117–120.

[12] E. Wigner
On the quantum correction for thermodynamic equilibrium
Phys. Rev., vol. 40, pp. 749–759, Jun. 1932.

[13] J. Ville
Theorie et applications de la notion de signal analytique
Cables et Transmiss., vol. 2A, pp. 61–74, 1948, (Translated from French by I. Selin, "Theory and applications of the notion of complex signal," RAND Corporation Technical Report T-92, Santa Monica, CA, 1958).

[14] L. Cohen
Time-Frequency Analysis. Englewood Cliffs, NJ, USA: Prentice-Hall, 1995.

[15] G. Cornelia, M. Lucian, and R. Romulus
Detection and estimation of linear FM signals
In *Proc. IEEE Int. Symp. Signal, Circuits Syst.*, 2005, pp. 705–708.

[16] V. C. Chen and H. Ling
Time-Frequency Transforms for Radar Imaging and Signal Analysis, Norwood, MA, USA: Artech House, 2002.

[17] B. Boashash Ed.
Time-Frequency Signal Analysis and Processing: A Comprehensive Reference, 2nd ed. Amsterdam, The Netherlands: Elsevier, 2003.

[18] F. Hlawatsch
Interference terms in the Wigner distribution
In *Proc. Int. Conf. Digit. Signal Process.*, 1984, pp. 363–367.

[19] D. C. Schleher
LPI radar: Fact or fiction
IEEE Aerosp. Electron. Syst. Mag., vol. 21, no. 5, pp. 3–6, May 2006.

[20] F. G. Geroleo and M. Brandt-Pearce
Detection and estimation of LFMCW radar signals
IEEE Trans. Aerosp. Electron. Syst., vol. 48, no. 1, pp. 405–418, Jan. 2012.

[21] S. O. Piper
Homodyne FMCW radar range resolution effects with sinusoidal nonlinearities in the frequency sweep
In *Proc. IEEE Int. Radar Conf.*, 1995, pp. 563–567.

[22] B. Boashhash and P. J. Black
An efficient real-time implementation of the Wigner-Ville distribution
IEEE Trans. Acoust., Speech Signal Process., vol. ASSP-35, no. 11, pp. 1611–1618, Nov. 1987.

[23] S. Kay and G. F. Boudreaux-Bartels
On the optimality of the Wigner distribution for detection
In *Proc. IEEE Int. Conf. Acoust., Speech, Signal Process.*, Tampa, FL, USA, 1985, pp. 27.2.1–27.2.4.

[24] B. Carlson, E. Evans, and S. Wilson
Search radar detection and track with the Hough transform. I. System concept
IEEE Trans. Aerosp. Electron. Syst., vol. 30, no. 1, pp. 102–108, Jan. 1994.

[25] T. O. Gulum, A. Y. Erdogan, T. Yildirim, and L. Durak-Ata
"Parameter extraction of FMCW modulated radar signals using Wigner-Hough Transform
In *Proc. IEEE 12th Int. Symp. Comput. Intell. Informat.*, 2011, pp. 465–468.

[26] T. O. Gulum, A. Y. Erdogan, T. Yildirim, and P. E. Pace
A parameter extraction technique for FMCW radar signals using Wigner-Hough-Radon transform
In *Proc. IEEE Radar Conf.*, 2012, pp. 0847–0852.

[27] A. Y. Erdogan, T. O. Gulum, T. Yildirim, L. Durak-Ata, and P. E. Pace
Defining the effective threshold using modified Wigner-Hough transform in FMCW signal detection
In *Proc. IEEE 21st Signal Process. Commun. Appl. Conf.*, 2013, pp. 1–4.

[28] T. O. Gulum, P. E. Pace, and R. Cristi
Extraction of polyphase radar modulation parameters using a Wigner-Ville distribution-Radon transform
In *Proc. IEEE Int. Conf. Acoust. Signal Process.*, 2008, pp. 1505–1508.

[29] D. Malnar, V. Sucic, and Z. Car
Optimizing the reference signal in the Cross Wigner-Ville distribution based instantaneous frequency estimation method
In *Proc. DAAAM Int. Symp. Intell. Manuf. Autom.*, 2014, vol. 100, pp. 1657–1664.

[30] T. K. Hon, A.F. Gonzalez, and A. Georgakis
Enhancing the readability of the Wigner distribution by exploiting its cross-terms geometry
In *Proc. IEEE Int. Conf. Acoust., Speech Signal Process.*, 2013, pp. 6254–6258.

[31] R. Watson
Use one figure of merit to compare all receivers
Microw. RF, vol. 26, no. 1, pp. 99–102, 1987.

[32] J. B. Y. Tsui, R. L. Shaw, and R. L. Davis
Performance standards for wideband EW receivers
Microw. J., vol. 32, no. 1, p. 46–54, 1989.

[33] J. Tsui
Digital Techniques for Wideband Receivers, 2nd ed. Raleigh, NC, USA: SciTech Publishing, 2004.

[34] A. Y. Erdogan, T. O. Gulum, L. Durak-Ata, T. Yildirim, and P. E. Pace
Digital chirp rate adaptation for increased FMCW interception performance in Hough based transforms
In *Proc. Radar Conf.*, 2014, pp. 1–5.

A. Yasin Erdogan (S'12–M'16) received the B.S. degree from Turkish Naval Academy, Istanbul, Turkey, in 1998, the M.S. degree from Naval Postgraduate School, Monterey, CA, USA, in 2004, and the Ph.D. degree from Yildiz Technical University, Istanbul, in 2015, all in electrical and computer engineering.

He is currently working for the Turkish Naval Research Center Command (TNRCC), Istanbul, as the Chief Engineer. He is mainly working on sensor, weapon, command and control development, and integration projects. Prior to his assignment to TNRCC, he served four years onboard naval platforms as a Commissioned Officer. His current research interests include radar signal processing, EW, EW systems, noise radar, and time-frequency analysis.

Taylan O. Gulum (S'12–M'15) received the B.S. degree from Turkish Naval Academy, Istanbul, Turkey, in 2001, the M.S. degree from Naval Postgraduate School, Monterey, CA, USA, in 2007, and the Ph.D. degree from Yildiz Technical University, Istanbul, in 2016, all in electrical and computer engineering.

He is currently working for the Turkish Naval Research Center Command (TNRCC), Istanbul, mainly in electronic warfare systems development and integration projects, radar cross section (RCS) measurement and analysis campaigns. Prior to his assignment to TNRCC, he served four years onboard naval platforms as a Commissioned Officer. His current research interests include RCS measurement, test, estimation and analysis, ship radar signature management, radar signal processing, EW systems and EW tactics, and time-frequency signal analysis.

Lutfiye Durak-Ata (S'93–M'04–SM'10) received the B.Sc., M.Sc., and Ph.D. degrees in electrical and electronics engineering from the Department of Electrical and Electronics Engineering, Bilkent University, Ankara, Turkey, in 1996, 1999, and 2003, respectively.

She worked in the Statistical Signal Processing Laboratory of Korean Advanced Institute of Science and Technology (KAIST) until 2005. She worked in the Department of Electronics and Communications Engineering, Yildiz Technical University, Istanbul, Turkey, from 2005 to 2015. She was a Visiting Research Scholar in the Department of Electrical and Computer Engineering, University of Pittsburgh, in 2008. Since September 2015, she has been working in Informatics Institute, Istanbul Technical University, Maslak, Turkey, where she is currently a Full Professor. Her research interests include time-frequency signal processing, statistical and adaptive signal processing and communications theory.

Dr. Durak-Ata is a member of the EURASIP and one of the Local Liaison Officers of Turkey since 2009.

Tülay Yildirim (M'08) received the B.S. and M.S. degrees in electronics and communication engineering from Yildiz Technical University (YTU), Istanbul, Turkey, in 1990 and 1992, respectively, and the Ph.D. degree in electrical and electronics engineering from the University of Liverpool, Liverpool, U.K., in 1997.

She is currently a Full Professor at YTU. Her current research interests include analog and digital integrated circuit design, hardware implementations of neural networks, medical electronics, biometrics, and artificial intelligence.

Phillip E. Pace (S'87–M'90–SM'97–F'17) received the B.S. and M.S. degrees from the Ohio University, Athens, OH, USA, in 1983 and 1986, respectively, and the Ph.D. degree from the University of Cincinnati, Cincinnati, OH, USA, in 1990, in electrical and computer engineering.

He is currently a Professor in the Department of Electrical and Computer Engineering, Naval Postgraduate School (NPS), Monterey, CA, USA. Prior to joining NPS, he spent two years at General Dynamics Corporation as a Design Specialist in the Department of Radar Systems Research Engineering. Before that, he was a Member of the Technical Staff at Hughes Aircraft Company, Radar Systems Group, for five years. He is the current Director for the NPS Center for Joint Services Electronic Warfare. He is the author of two textbooks and has co-authored two papers.

Dr. Pace received the Hughes Aircraft Company Full Study Fellowship in 1984, was the winner of the Kroeger Foundation Fellowship Award in 1989, and was presented with the Outstanding Graduate Researcher of the Year Award in 1990 for his Ph.D. work in signal processing and computing. He was also selected for the Outstanding Research Achievement Award in 1994 and 1995 for his work at the NPS in electronic warfare and received the Association of Old Crows 1995 Academic Training Award. He has been the Chairman of the Navy's Threat Simulator Validation Working Group since October 1998 and was a participant on the Navy's NULKA Blue Ribbon Panel in January 1999. He was also selected as an electronic warfare program review panel member in 2007 for the Office of Naval Research. His two papers received the Best Paper Award-Electronic Warfare (WG-9) in the Military Operations Research Society Symposium in 1995 and 2004. He has been a Principal Investigator on numerous research projects in the areas of superconducting and optical signal processing, electronic warfare, and weapon systems analysis. He is a member of the Eta Kappa Nu, a Life Member of the AOC, and an Associate Editor for IEEE TAES.